Smooth approximation of potential fields from noisy scattered data

Michael Rauth* and **Thomas Strohmer**†

(February 12, 1997)

ABSTRACT

Geophysical potential-field data are in general observed at scattered sampling points and are contaminated by measurement and preprocessing errors. Analysis and further treatment require a representation of the underlying potential fields on a regular grid. In the presence of noise an approximation of the data is more appropriate than an exact interpolation. Analysis of the smoothness of potential fields indicates an approximation by band-limited functions. The resulting least squares problem can be formulated as a linear system of equations, where the system matrix is of block-Toeplitz type. This special structure allows a computationally attractive and robust solution via the Fast Fourier transform and the conjugate gradient algorithm. Based on this we present a gridding method that incorporates additional knowledge about the physical properties of potential fields and the statistics of the data. Experimental results for synthetic and real world gravity data demonstrate good performance for highly irregularly spaced noisy data.

INTRODUCTION

In geophysical practice it is essentially impossible to gather data in a form that allows direct interpretation. Geoscientists, used to looking at their measurements on maps or profiles and aiming at further processing, therefore need a representation of the originally irregularly spaced (scattered) data points at a regular grid. Gridding is thus one of the first and crucial steps in data analysis, and a variety of problems must be taken into account as already indicated by Cordell (1992):

1. Anisotropies in the sampling set make the right choice of the grid interval difficult, as it may be too small in areas of sparse control but too big in regions of data clusters.

2. As measurements are never exact, one should not try to interpolate the data, but rather find an approximation by fitting the error envelope.

3. If the underlying physical process of the data is known, this additional information should be incorporated into the gridding process.

4. The dimensionality of the problem must be considered, i.e. data with a big variation in altitude should be gridded with a 3-D method rather than with a 2-D algorithm.

5. Additionally more practical requirements to an algorithm arise from the limited computational time and memory storage, if one deals with large data sets.

A variety of gridding methods can be found in the literature. The following references are a representative but not complete list of existing gridding algorithms. For a review on scattered data interpolation see e.g. Foley and Hagen (1994) and the references given there. In the exploration potential field community the minimum-curvature interpolation (Briggs, 1974; Webring, 1981) is very often the method of choice, although it only deals with item 5 and to a certain extend with item 3, as the interpolant is the "smoothest" surface passing through the samples.

More modern methods like the generalized equivalent-source method (Cordell, 1992) or kriging (Hansen, 1993) address more of the problems mentioned above, but have also their drawbacks, as the unsatisfactory behavior of the solution in areas of sparse control of the former, or the high computational costs and dependence of adjustable parameters of the latter.

The method developed in this papers is a computationally efficient and robust 2-D method for smooth approximation of highly irregularly sampled potential field data in the presence of noise, thus addressing items 1-3 and 5 of the list above. Since the proposed method can be generalized to higher dimensions, it could in principle also address item 4.

The paper is divided into a theoretical and an experimental part. In the first part we show that potential fields satisfy certain smoothness properties. It is demonstrated how potential fields can be approximated by trigonometric polynomials. We then present the algorithm and give details about a numerical implementation. The second part is devoted to experimental results. A synthetic example will be used to study the performance of the new method and a real world example treats gravity data from the eastern part of Austria.

THEORY

We first demonstrate that the gravity and the magnetic field are so-called essentially band-limited functions. Since functions of that type can be well approximated by strictly band-limited functions, we can use

*Department of Geophysics, University of Vienna, Nordbergstr.17, A-1090 Wien, Austria
†Department of Mathematics, University of Vienna, Strudlhofg.4, A-1090 Wien, Austria

methods originally developed for the irregular sampling problem of band-limited functions, to design an efficient algorithm for the approximation of the gravity and the magnetic field.

For a precise description of the problem, suppose that we have a set of r distinct irregularly distributed sampling points $\mathbf{x}_j = (x_1, x_2)$ in an interval, say $[0, N) \times [0, N)$, and sampling values $s_j = f(\mathbf{x}_j) + \epsilon_j$, where f is the underlying potential function and ϵ_j the error arising from imperfect measurements or preprocessing. Since we are developing a 2-D method, we implicitly assume all sampling points at a constant altitude x_3.

The task is to find a reasonable and computable approximation of f on a finite and discrete set of regularly spaced grid points $\mathbf{\Delta} = \{(\Delta_1, \Delta_2)\}$ for $\Delta_{1,2} = 0, \ldots, N-1$. Choosing the interval of regular grid points as square is no loss of generality, since all other intervals can be obtained by simple rescaling.

Smoothness of potential fields

A characteristic of potential fields away from discontinuities, such as sources, is that the overall appearance is "smooth". In this section we demonstrate that this smoothness property can be described by the concept of so-called essentially band-limited functions.

Let $\hat{f}$ denote the continuous 2D-Fourier transform of the function f defined by

$$\hat{f} = \int_{-\infty}^{\infty} f e^{-i\mathbf{v}\cdot\mathbf{x}} d\mathbf{x}, \tag{1}$$

where $\mathbf{x} = (x_1, x_2)$ and $\mathbf{v} = (v_1, v_2)$ are the spatial and the angular frequency coordinates respectively, $\mathbf{v} \cdot \mathbf{x} = v_1 x_1 + v_2 x_2$, and i denotes the imaginary unit. Further we write $\mathbf{v}^*$ for the conjugate transpose of $\mathbf{v}$, and denote the length or Euclidean norm of $\mathbf{v}$ by $\|\mathbf{v}\| = \sqrt{v_1^2 + v_2^2}$.

From potential theory it is well known that the continuous Fourier transform of a gravitational potential U caused by a density distribution $\rho(\xi_k)$ at a point $\mathbf{x} = (x_k)$, $k = 1, 2, 3$, above the distribution is given by (Bhattacharyya, 1966; Gunn, 1975)

$$\hat{U} = 2\pi G \int_{-\infty}^{x_3} \hat{\rho} \, \frac{e^{-(x_3 - \xi_3)\|\mathbf{v}\|}}{\|\mathbf{v}\|} \, d\xi_3, \tag{2}$$

where G is the gravitational constant and x_3 is positive upwards.

In practice one usually measures the vertical component of the gravitational acceleration g_3. Its representation in the frequency domain can be derived by differentiating equation (2) with respect to ξ_3:

$$\hat{g}_3 = 2\pi G \int_{-\infty}^{x_3} \hat{\rho} \, e^{-(x_3 - \xi_3)\|\mathbf{v}\|} \, d\xi_3. \tag{3}$$

Similar expressions hold for the magnetic potential V: Let $m(\xi_k)$ be a magnetic distribution. Let L_k and l_k be the direction cosines of the direction of magnetization and of the component being measured respectively. Introducing the abbreviations

$$\begin{aligned} \bar{L} &= iL_1 v_1 + iL_2 v_2 + L_3 \|\mathbf{v}\| \\ \bar{l} &= il_1 v_1 + il_2 v_2 + l_3 \|\mathbf{v}\| \end{aligned}$$

the potential $\hat{V}$ and the field intensity $\hat{M}$ in the frequency domain can be written as

$$\hat{V} = 2\pi \bar{L} \int_{-\infty}^{x_3} \hat{m} \, \frac{e^{-(x_3 - \xi_3)\|\mathbf{v}\|}}{\|\mathbf{v}\|} \, d\xi_3 \tag{4}$$

and

$$\hat{M} = 2\pi \bar{L} \, \bar{l} \int_{-\infty}^{x_3} \hat{m} \, \frac{e^{-(x_3 - \xi_3)\|\mathbf{v}\|}}{\|\mathbf{v}\|} \, d\xi_3. \tag{5}$$

With the assumption that the sources $\rho(\xi_k)$ and $m(\xi_k)$ are restricted to a localized region below the plane of measurement, i.e. $x_3 > \xi_3$, it follows that the integrals in equations (3) and (5) exist and are also finite.

Thus we can conclude that the magnitude of the spectrum of the gravity and the magnetic field decay exponentially with increasing frequency index $\mathbf{v}$. In other words, the contribution of high frequencies is negligible in some sense. Functions with this property belong to a larger class, the so-called essentially band-limited functions. We define the space of 2-D *essentially* Ω*-band-limited* functions $\mathcal{B}_{\Omega,\delta}$ by

$$\mathcal{B}_{\Omega,\delta} = \left\{ f : \int_{\mathbf{v} > \Omega} |\hat{f}(\mathbf{v})|^2 d\mathbf{v} \le \delta^2 \|f\|^2 \right\},$$

where δ is a small number. A function is called strictly Ω-band-limited (or simply band-limited) if $\delta = 0$.

It is well-known that a band-limited function can be reconstructed from its (uniformly or non-uniformly spaced) sampling values, if the sampling points satisfy some density criterion, cf. Feichtinger and Gröchenig (1994) and Higgins (1996). If f is an essentially band-limited function, it cannot be completely reconstructed from its sampling values. If we compute f nevertheless from its samples we commit an error, the so-called *aliasing error*. An estimate for the error of approximating essentially band-limited functions by strictly band-limited functions will be given in equation (13) in the next section.

In the sequel we present an efficient method for the reconstruction of 2-D band-limited functions and show how the method can be easily adapted to the reconstruction of potential fields.

Approximation by trigonometric polynomials

The analysis of the discrete nonuniform sampling problem of band-limited functions suggests an approximation of the continuous band-limited function f by *trigonometric polynomials* (Gröchenig, 1994; Feichtinger et al., 1995).

Thus for any integer $M > 0$ we consider the $(2M+1)^2$-dimensional space $\mathcal{P}_M$ of 2-D trigonometric polynomials of degree M^2

$$p(\mathbf{x}) = \sum_{\mathbf{v}=-M}^{M} c_{\mathbf{v}} e^{2\pi i \mathbf{v}\cdot\mathbf{x}/N^2} \tag{6}$$

where the coefficients $c_{\mathbf{v}}$ uniquely determine p. For simplicity of representation we assume that the trigonometric polynomials have the same number of coefficients in both frequency coordinates. Clearly all results in this paper hold for trigonometric polynomials with a different number of coefficients in the frequency coordinates.

To avoid unnecessary introduction of new variables we slightly abuse our notation by treating the $(2M+1) \times (2M+1)$ array c also as a vector by stacking the columns of c.

We look for a trigonometric polynomial $p \in \mathcal{P}_M$ with $(2M+1)^2 \le r$ that approximates f at the given (user-defined) set $\mathbf{\Delta}$ of regularly spaced grid points. Two questions arise immediately:
(i) How can we compute the optimal polynomial for a given M?
(ii) How can we determine the optimal choice of M?

To answer the first question we consider the following least squares problem: Given the samples as defined above, weights $w_j > 0$, and the degree of the polynomial, we want to find a polynomial $\tilde{p}$ that solves

$$\min \sum_{j=1}^{r} |s_j - p(\mathbf{x}_j)|^2 w_j \tag{7}$$

where the minimum is taken over all trigonometric polynomials $p \in \mathcal{P}_M$. The reason for the introduction of the weights w_j will be explained at the end of this section.

The second-named author has shown that the coefficients $\tilde{c}$ of the trigonometric polynomial $\tilde{p}$ can be computed by solving the linear system of equations $T\tilde{c} = b$ with the following algorithm (Strohmer, 1996):

Algorithm 1
Input: Sampling points $\mathbf{x}_j$, sampling values s_j, the weights w_j, and the degree M^2 of the polynomial.
Step 1: Compute the entries of T and b by

$$T_{\mathbf{vu}} = \sum_{j=1}^{r} w_j e^{2\pi i(\mathbf{v}-\mathbf{u})\cdot\mathbf{x}_j/N^2} \tag{8}$$

$$b_{\mathbf{v}} = \sum_{j=1}^{r} w_j s_j e^{2\pi i \mathbf{v}\cdot\mathbf{x}_j/N^2} \tag{9}$$

for $|v_1|, |v_2|, |u_1|, |u_2| \le M$.
Step 2: Solve

$$\tilde{c} = T^{-1} b \tag{10}$$

Step 3: Compute

$$\tilde{p}(\mathbf{x}) = \sum_{\mathbf{v}=-M}^{M} \tilde{c}_{\mathbf{v}} e^{2\pi i \mathbf{v}\cdot\mathbf{x}/N^2}. \tag{11}$$

This algorithm is essentially based on the so-called *ACT*-method proposed in Feichtinger et al. (1995). In the rare situations where T is not invertible, the least squares solution of $\min \|T\tilde{c} - b\|$ can be computed via the pseudo-inverse of T (Golub and van Loan, 1996).

It is crucial for the proposed fast algorithm that T is a *block Toeplitz matrix*, i.e. T is of the form

$$T = \begin{bmatrix} B_0 & B_1 & \cdots & B_{N-1} \\ B_{-1} & B_0 & \cdots & B_{N-2} \\ \vdots & \vdots & & \vdots \\ B_{-N+1} & B_{-N+2} & \cdots & B_0 \end{bmatrix} \tag{12}$$

where each B_i itself is a Toeplitz matrix, i.e. the entries of B_i are constant down each diagonal, see Strohmer (1996). An important advantage of block Toeplitz matrices is that they can be inverted with considerably less computational effort than matrices without special structure. Linear algebra provides a large repertory of Toeplitz- and block-Toeplitz solvers (Robinson and Treitel, 1980; Ammar and Gragg, 1988; Strang, 1986; Bitmead and Anderson, 1980). Depending on the size of T and the required precision one may choose either *direct* methods for the complete inversion of T or *iterative* methods for an approximation of T^{-1}. We return to this question in the next section.

The aliasing error for approximating a potential field f from its samples $f(\mathbf{x}_j)$ on a regular grid $\mathbf{\Delta}$ by Algorithm 1 can be estimated by

$$\|f(\mathbf{\Delta}) - \tilde{p}(\mathbf{\Delta})\| \le \sqrt{\delta(1+\lambda^{-1})}\|f(\mathbf{\Delta})\| \tag{13}$$

where λ is the minimal eigenvalue of the matrix T (Strohmer, 1996).

The introduction of the weights $\{w_j\}_{j=1}^{r}$ in equation (7) has been done for two reasons. If the sampling points $\mathbf{x}_j$ are very irregularly distributed in the sense that the sampling density is varying, the weights w_j can compensate for these irregularities in the sampling set. As a rule of thumb sampling values in sparse sampled regions are considered as more important and thus get a larger weight, whereas samples in densely sampled regions get a smaller one. A proper choice of weights speeds up the rate of convergence, see Feichtinger and Strohmer (1993) and Strohmer (1996) for details and for an efficient strategy of determining proper weights.

Moreover the weights w_j allow to incorporate information about varying quality of the measurements s_j, caused e.g. by the use of instruments with different precision. This information can be included in our method in a straightforward way, by assigning smaller weights to less precise and larger weights to more accurate measurements.

Adaptation of the algorithm to the approximation of potential fields

In Algorithm 1 we compute the solution $\tilde{p}$ of $\min \sum_{j=1}^{r} |s_j - p(\mathbf{x}_j)|^2 w_j$ in order to approximate f by $\tilde{p}$ at a given set $\mathbf{\Delta}$. However the fact that $\tilde{p}$ is the optimal solution of (7) for a fixed M does not necessarily imply that $\tilde{p}$ is also the optimal solution for $\min \|f - p\|$ or $\min \|f(\mathbf{\Delta}) - p(\mathbf{\Delta})\|$, especially since the samples s_j are in general contaminated by noise. Clearly we cannot compute the optimal solution of $\min \|f(\mathbf{\Delta}) - p(\mathbf{\Delta})\|$ for a given M, but we can improve our approximation $\tilde{p}$ by using further knowledge about the original function f. This can be done in the following way: We look for a polynomial $\bar{p}$ which is close to the minimum $\tilde{p}$ in the sense that

$$\sum_{j=1}^{r} |\bar{p}(\mathbf{x}_j) - s_j|^2 w_j \approx \sum_{j=1}^{r} |\tilde{p}(\mathbf{x}_j) - s_j|^2 w_j,$$

but we do not force $\bar{p}$ to be the optimal solution of (7). Instead we make use of our specific knowledge about the exponential decay of the frequency components of potential fields to compute $\bar{p}$ and require that the coefficients $\bar{c}$ of $\bar{p}$ resemble the shape of potential field spectra.

A simple but efficient technique to incorporate this knowledge is the following: The solution $\tilde{c}$ of equation (10) can be found by minimizing $\|Tc - b\|$. Instead of using the standard Euclidean norm $\|.\|$, we introduce a so-called weighted Euclidean norm $\|.\|_d$ by

$$\|z\|_d^2 = \sum_{\mathbf{k}=-M}^{M} |z_{\mathbf{k}}|^2 d_{\mathbf{k}}^2 \,, \tag{14}$$

where the weights are given by

$$d_{\mathbf{k}} = e^{-\|\mathbf{k}\|} \,, \tag{15}$$

and resemble the shape of the spectrum of the fields under consideration, cf. equations (3) and (5).

Treating d as vector by stacking its columns, we define the diagonal matrix D by $D = \mathrm{diag}(d)$. The minimum of $\|Tc - b\|_d$ in the new norm is equivalent to the minimum of $\|DTc - Db\|$ in the standard Euclidean norm, and we compute the polynomial $\bar{p}$ whose coefficients $\bar{c}$ solve

$$\min \|DTc - Db\| \,. \tag{16}$$

Solving the scattered data problem with respect to the weighted norm, equation (14), can be seen as regularizing the solution in presence of noise. This regularization allows to control undesirable overshoots and undershoots of the approximation by keeping the influence of high frequencies small, and therefore increases the stability of the method.

Although the functional relationship of equation (15) looks like the filter for upward continuation, it is important to note that it has a completely different meaning here and should not be confused with the latter.

Numerical Implementation

The question arises how to solve (16) fast and stable. The *conjugate gradient method* (CG) is known as an efficient iterative method to solve linear systems of equations (Hageman and Young, 1981) and it is particularly well suited for Toeplitz-like systems (Strang, 1986; Chan and Strang, 1989). A detailed discussion of CG can be found for instance in Golub and van Loan (1996).

Observe that we do not interpret the application of D as preconditioning, since we do neither expect that DT has a lower condition number than T nor that DT has better clustered eigenvalues. However formally the use of a weighted norm via applying D and the application of a preconditioner can be handled similarly. Thus we can directly apply the formulas for the *preconditioned conjugate gradient method* (PCG) to solve (16).

In the sequel we present our algorithm for the reconstruction of a potential field f from scattered data, based on Algorithm 1 and PCG.

Algorithm 2
Input: Sampling points $\mathbf{x}_j$, the sampling values s_j, the weights w_j, $j = 1, \ldots, r$, the accuracy threshold tol, and the degree M^2 of the polynomial, such that $r \geq (2M+1)^2$.
Step 1: Compute T and b as defined in Algorithm 1 and the entries of D as defined in (15).
Step 2: Initialize $r_0 = b, c_0 = 0, n = 0$ and compute $\bar{c}$ iteratively:

$$
\begin{aligned}
&\textbf{while } \; accurate > tol \\
&\quad z_n = D r_n \\
&\quad n = n + 1 \\
&\quad \textbf{if } \; n = 1 \\
&\quad\quad q_1 = z_0 \\
&\quad \textbf{else} \\
&\quad\quad \beta_n = r_{n-1}^* z_{n-1} / r_{n-2}^* z_{n-2} \\
&\quad\quad q_n = z_{n-1} + \beta_n q_{n-1} \\
&\quad \textbf{end} \\
&\quad \alpha_n = r_{n-1}^* z_{n-1} / q_n^* T q_n \\
&\quad c_n = c_{n-1} + \alpha_n q_n \\
&\quad r_n = r_{n-1} - \alpha_n T q_n \\
&\textbf{end} \\
&\bar{c} = c_n
\end{aligned}
$$

Step 3: The solution $\bar{p}$ is then given by

$$\bar{p}(\mathbf{x}) = \sum_{\mathbf{v}=-M}^{M} \bar{c}_{\mathbf{v}} e^{2\pi i \mathbf{v}\cdot\mathbf{x}/N^2} \tag{17}$$

for $v_1, v_2 = 0, \ldots, N-1$.

Several choices for the stopping procedure *accurate* can be found in the literature (Hageman and Young, 1981). Since we want to fit the error envelope of the data, a suitable criterion for our situation is to stop the iterations as soon as the error of the approximation at the sampling points becomes smaller than the measurement error.

Complexity of the algorithm: Due to the block-Toeplitz structure the whole information of T is stored in the first and M-th column of T. Hence the computational effort for the calculation of the relevant entries of T and b in Step 1 is of order $\mathcal{O}(rM^2)$ operations. In Beylkin (1995) a fast algorithm has been proposed for the approximative evaluation of trigonometric sums of the form (8) and (9). This algorithm allows to reduce the computational complexity of Step 1 to $\mathcal{O}(M^2 \log M + r(\log 1/\varepsilon)^2)$, where ε is the precision for computing T and b.

The main effort in Step 2 is one matrix-vector multiplication in each iteration. It is essential for the efficiency in terms of speed and memory of the proposed algorithm that multiplication of a vector by the block-Toeplitz matrix T can be computed using 2-D FFT, analogous to Toeplitz matrices, see Strang (1986). Thus the computational effort of Step 2 is $\mathcal{O}(\kappa M^2 \log M)$ operations where κ is the number of iterations.

Equation (17) in Step 3 can be evaluated in $\mathcal{O}(N^2 \log N)$ operations by defining $\bar{c}_{\mathbf{v}} = 0$ for $M+1 \le |v_1|, |v_2| \le N/2$ and replacing (17) by

$$\bar{p}(\mathbf{x}) = \sum_{\mathbf{v}=-N/2}^{N/2-1} \bar{c}_{\mathbf{v}} e^{2\pi i \mathbf{v}\cdot\mathbf{x}/N^2} . \tag{18}$$

Since the points $\mathbf{v}$ are regularly spaced, equation (18) can be computed by a 2-D FFT.

Trigonometric polynomials are periodic functions, thus our approximation is periodic at the boundaries. A potential field is in general not periodic. Thus our reconstruction will show some artifacts at the boundaries. However, these artifacts can be reduced by choosing the regular grid $\mathbf{\Delta}$ somewhat larger than suggested by the data and reducing the resulting approximation to the original region of interest.

How to determine the optimal polynomial degree: We still have to solve the problem how to determine the optimal degree of the polynomial $\bar{p}$.

To find an answer to this question we bear in mind the two main conditions our approximation should satisfy:
(i) The polynomial $\bar{p}$ has to fit the samples s_j at the points $\mathbf{x}_j$ (at least up to the precision of the measurements);
(ii) $\bar{p}$ should be a smooth function without high oscillations.

These are two contrary conditions: If we want to satisfy condition (i), we have to choose a large degree for $\bar{p}$, since the samples s_j are contaminated by noise and f is not strictly band-limited. However a large degree may result in a highly oscillating function, which is in conflict with the second condition. But if we choose a low degree for $\bar{p}$, we may get a large deviation at the samples in contradiction to condition (i).

We use following *cascadic* scheme to find the "optimal" balance between these two conditions: Starting from a small value of M_0 we run Algorithm 2 until a certain stopping criterion is satisfied. After the iteration is stopped at scale M_0, we test by a *discrepancy principle* if the last iterate $\bar{p}_{M_0}$ is acceptable as an approximation of the desired solution. This is done by calculating the error at the samples $\|\bar{p}_M(\mathbf{x}_j) - s_j\|$ and comparing it to the error envelope of the data. If the discrepancy principle is satisfied, the process is stopped, otherwise $\bar{p}_{M_0}$ is used as an initial guess at a finer scale, i.e. for a larger value of M. We proceed inductively until the discrepancy principle is satisfied, to learn the appropriate essential bandwidth of the underlying potential field.

Clearly this procedure increases the computational effort, because we have to run the algorithm several times for different choices of M. But fortunately the additional amount can be kept small, which is due to following observations. The entries of T can be calculated successively for increasing M, since the matrix T for a spectrum of size M contains all block Toeplitz matrices for smaller choices of M as sub-matrices and only the additional elements have to be determined. The same holds true for the entries of b. Although this procedure provides good results, one of our future aims is to find a more simple method to estimate the bandwidth of potential fields from noisy scattered data.

We refer to (Scherzer, 1996) for appropriate stopping criteria for cascadic algorithms, a detailed discussion would be beyond the scope of this paper. A mathematically rigorous description of cascadic algorithms for the reconstruction of band-limited signals will be presented in a forthcoming joint paper of O. Scherzer and the second-named author.

EXPERIMENTAL RESULTS

In this section we study the performance of the proposed method by reconstructing a synthetic gravitational anomaly. We also show an application to real gravity data from the eastern part of Austria.

The algorithm has been implemented in MATLAB, a high level interpreter language, ideally suited for the development of new algorithms. As the practical performance and efficiency of an algorithm depend very much on the coding, the computer language, optimization during compilation, and to a big extend on the hardware, we present the number of iterations and other relevant parameters for the estimation of the complexity of the algorithm rather than execution times.

A detailed numerical comparison of our algorithm with the well established ones mentioned in the introduction is beyond the task of this paper and will be done in an upcoming study. Nevertheless we also used minimum curvature to grid one of our test examples for a first comparison.

A synthetic test example

Our synthetic anomaly represents the gravitational acceleration due to an ensemble of buried rectangular boxes

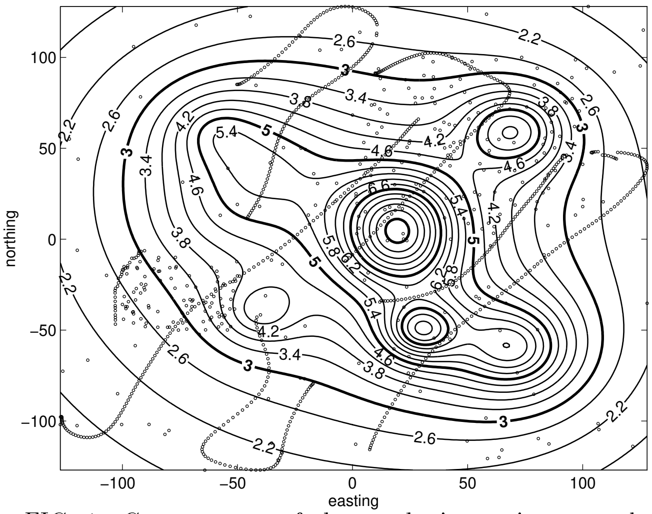

FIG. 1. Contour map of the synthetic gravity anomaly. Gravity is in mGal, contour interval is 0.4 mGal. Also shown is the sampling set of 1000 points, indicated by small circles. Coordinates are easting and northing, units are in m.

of different size, depth, and density contrast.

This anomaly was then sampled at a highly irregularly distributed set of 1000 sampling points. The sampling geometry is depicted together with the contour plot of the original anomaly evaluated at the grid points in Figure 1. Note that this set is composed of a line type sampling set, which is characteristic for airborne or other fast moving measuring devices, clusters and a pure random part. Thus there is a severe anisotropy in the spatial data density. We chose this sampling set since it shows all features which are typical for real-world settings, as can be seen from the example of the Neusiedlersee area (see Figure 4 below).

As real world measurements have always a certain amount of error, we added white noise with an amount of 1% to 20% of the energy $\|s\|$ of the sampling set. Since all data were of the same accuracy, we did not use weights, which is equivalent to assigning the sample s_j a weight $w_j = 1$.

We then reconstructed the anomaly from the samples on a grid of the size 256×256 and a spacing of 1m. To measure the quality of the approximation, the relative deviation of the reconstructed anomaly from the original one evaluated at the grid points in percent has been calculated via

$$\frac{\|\bar{p}(\boldsymbol{\Delta}) - f(\boldsymbol{\Delta})\|}{\|f(\boldsymbol{\Delta})\|} \cdot 100. \tag{19}$$

To allow a comparison in mGal, we also expressed the error in terms of the standard deviation σ.

As an example the contour plot of the reconstructed anomaly with 5% noise is depicted in Figure 2a. Figure 2b shows the error of the reconstruction. The dependence of the approximation error as a function of the amount of noise together with the degree of the polynomial and the number of iterations is given in Table 1. For the depicted example the complexity of the algorithm translates into an execution time of 39 seconds on our Digital Alpha workstation 250/4.

The grid values range from 1.224 mGal to 9.088 mGal, the mean being 3.461 mGal. Comparing this to the values of the original anomaly evaluated at the grid points – which range from 1.514 mGal to 9.201 mGal with a mean of 3.487 mGal – we see that the deviation is slightly larger than one standard deviation σ of the error, being 0.199 mGal in this case. This is a satisfying result, as we reconstructed from the noisy samples that did not cover all details of the anomaly. The values of the approximation at the sampling points range from 1.341 mGal to 9.434 mGal with a mean of 3.791 mGal. If we compare that to the noisy sampling values, which have minimal and maximal values of 1.324 mGal and 9.283 mGal respectively and a mean of 3.677 mGal, we see that they coincide within the 1σ envelope.

Comparing the map of the approximation (Figure 2a) with the map of the original anomaly (Figure 1) we make the following observations: Both maps look very similar in the central part of the area, and all important features are well represented. The main difference between the two maps is on the boundary of the region, where the approximation shows some spurious features. These are caused by the periodicity of the approximation, as mentioned above.

TABLE 1. Approximation error for the test example

Noise		Degree	Iterations	Global error		Error at samples	
%	mGal	of $\bar{p}$		%	mGal	%	mGal
0	0.000	225	482	2.55	0.097	0.45	0.018
1	0.040	225	405	3.02	0.114	1.09	0.043
2	0.079	225	384	3.65	0.138	1.99	0.079
5	0.199	144	304	5.17	0.193	4.99	0.198
10	0.397	121	224	7.13	0.266	9.94	0.395
20	0.794	49	134	9.83	0.366	19.98	0.800

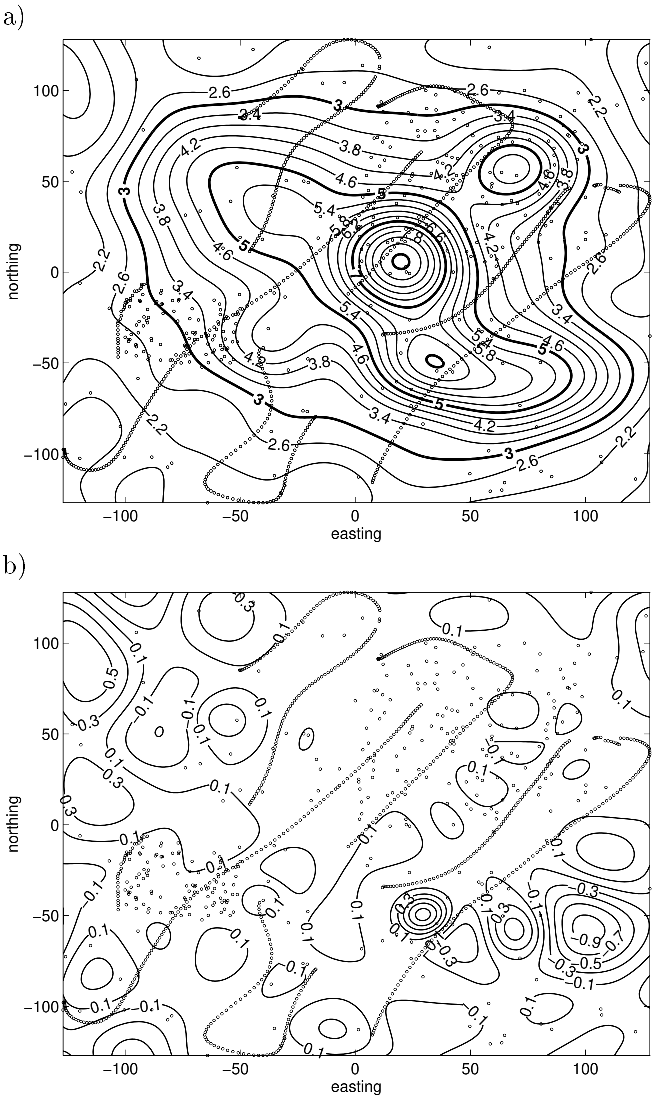

FIG. 2. a) Approximation of the original gravity anomaly (Fig.1) by Algorithm 2 from the samples after adding 5% of white noise. Contour interval is 0.4 mGal. b) Error between the approximation a) and the true anomaly (Fig.1) in mGal. Contour interval is 0.2 mGal. Sampling points are indicated by small circles. Gravity is in mGal. Coordinates are easting and northing, units in m.

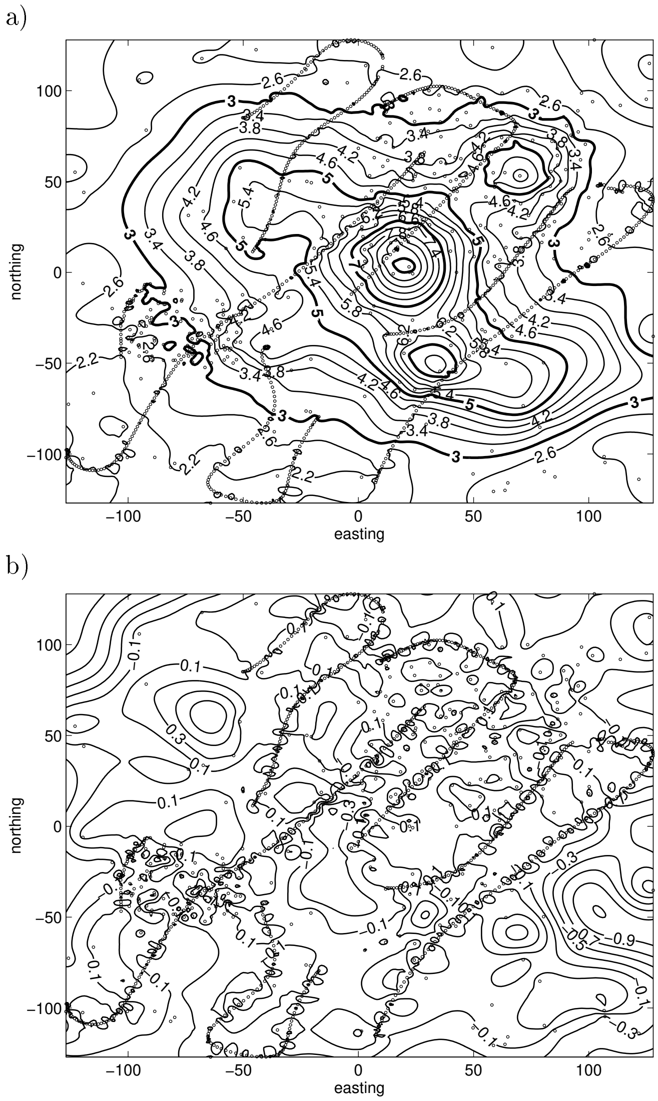

FIG. 3. a) Approximation of the original gravity anomaly (Fig.1) by minimum curvature from the samples after adding 5% of white noise. Contour interval is 0.4 mGal. b) Error between the approximation a) and the true anomaly (Fig.1) in mGal. Contour interval is 0.2 mGal. Sampling points are indicated by small circles. Gravity is in mGal. Coordinates are easting and northing, units in m.

The boundary effects also appear in the contour plot of the approximation error (Figure 2b), where it becomes obvious that the maximal error occurs in those regions on the boundary where no data are available, something one expects to happen. Note that the approximation is excellent in the central part of the region, where the only two bigger deviations from the original anomaly show up in regions of very local, small scale peaks with an amplitude of the size of the error.

To demonstrate the difference between our model based approximation and a pure interpolation, we also gridded the synthetic test example with 5% noise with the minimum curvature program of Webring (1981).

Figure 3a shows the contour plot of the resulting anomaly together with the sampling set. The error of the minimum curvature grid is depicted in Figure 3b. The global error as calculated by equation (19) is 6.75% or 0.252 mGal, which is considerably bigger than the error of the approximation by Algorithm 2, being 5.17% or 0.193 mGal in this case. A visual comparison of Figure 2a and Figure 3a shows that the approximation by Algorithm 2 is smoother than the interpolation by minimum curvature, especially in areas of high sampling density. The interpolating nature of the minimum curvature algorithm forces the solution to pass through the noisy samples. This becomes even more evident if we consider the error between the minimum curvature grid and the original anomaly (Figure 3b), which strongly correlates with the sampling set.

As far as the behavior of the approximation error of Algorithm 2 as a function of noise is concerned (Table 1), it is clear that also in the absence of noise there is an intrinsic error. This is due to the fact that not all features are sampled and we approximate an essentially band-limited function by a really band-limited one. The error increases linearly with increasing noise, until a point is reached where the noise is of the same magnitude as the periodicity error, and the method performs better and better. The global error augments then only to the proportion of small scale features which get lost in the noise level. Note that even for the case of 20% noise in the samples the global error is still only 9.8%.

From Table 1 it becomes clear that the size of the spectrum, expressed by the degree of the polynomial, becomes smaller with an increase of noise. This not only leads to a smoother approximation but also decreases the computational expenses, as only that part of the spectrum is calculated that still contains meaningful information.

Gravity data from the Neusiedlersee area

The Neusiedlersee is the largest lake in the eastern part of Austria. The area under consideration is 39 by 37 km with an average height of 132 m and a variation of 19.3 m. Gravity data comprise 989 stations. 99 of the measurements were taken along profiles on the frozen lake during the winter 1965/66. For survey specifications and an interpretation of the data, the interested reader is referred to Granser et al. (1991). The terrain-corrected Bouguer anomaly is based on a reduction density of 2.2 g/cm^3 as determined by Granser et al. We estimated the upper bound of the error due to elevation and terrain correction at 0.6 mGal. The data are in the range between -16.5 mGal and 3.1 mGal, with a mean of -5.0 mGal. We gridded the data on a 150m grid with our method. The gridded anomaly together with the sampling set is shown in Figure 4.

The approximating polynomial has degree 196 and the desired accuracy was obtained after 350 iterations. The regularization property of the frequency weights ensures that even this high degree of the polynomial does not result in a strongly oscillating approximation.

Grid values range from -15.9 mGal to 2.7 mGal with an average of -5.6 mGal, which is within the 1σ bound. The minimal and maximal values of the approximation at the sampling locations are -15.6 mGal and 2.7 mGal, respectively and the mean is -5.0 mGal. Thus the approximation undershoots local high station values and overshoots local low station values, which has the desired effect of reducing aliasing. Clearly it is not possible to give the true error, as the underlying potential is not known.

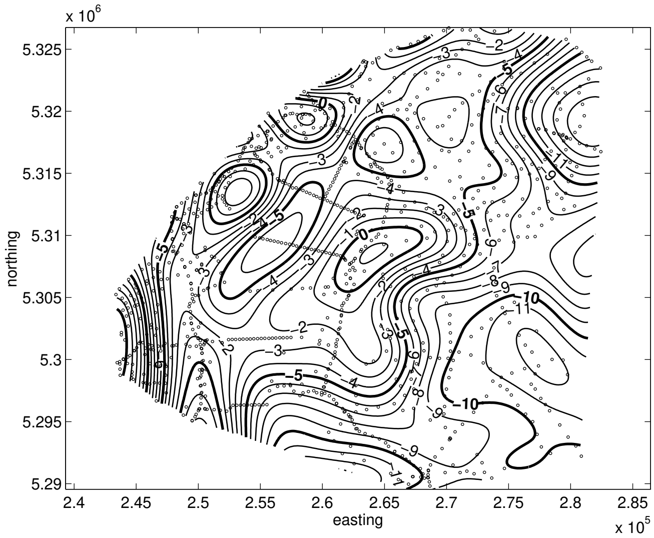

FIG. 4. Contour plot of the Bouguer gravity anomaly in the Neusiedlersee area (Austria). Gravity is in mGal, contour interval is 1 mGal. Also shown are sampling points, indicated by small circles. Coordinates are easting and northing, units in m.

DISCUSSION

The gridding method proposed in this paper shows a good performance for the approximation of potential field data from highly irregular sampling sets under the presence of noise. It is perhaps one of the first methods which addresses extremely anisotropic geometries, like line-type data, also incorporating the physical background of the process being measured, as well as having the capability to include statistical information, such as varying data quality, by easy means.

Furthermore the algorithm is in some sense of minimum complexity from a computational point of view, as it depends mainly on the number of samples and the size of the spectrum. The latter is small since the magnitude of the spectrum of the functions under considerations decay exponentially and the spectrum is truncated as soon as the level of noise is reached.

Especially for very noisy data our method will still reconstruct the low frequency part of the spectrum, and the resulting approximation will be smoother and thus physically more meaningful than any interpolation. The price one has to pay is the periodicity of the approximation, which may lead to unwanted and troublesome boundary effects.

We believe that our method is of strong practical relevance in the situations described above. Nevertheless we would like to stress that in general we do not consider our method to be superior to established methods like minimum curvature (which is in our opinion one of the best algorithms for gridding almost all scattered data sets) or the others mentioned in the introduction.

It is still the scientist who has to select the appropriate method to grid his data, depending on the actual geometry of the sampling set, the quality of the data and the resources available for processing.

ACKNOWLEDGMENTS

We wish to thank Dr. B. Meurers for providing the Neusiedlersee gravity data. The authors have been supported by the projects P10473-GEO and S7001-MAT of the Austrian Science Foundation FWF respectively.

REFERENCES

Ammar, G., and Gragg, W., 1988, Superfast solution of real positive definite Toeplitz systems: SIAM J. Matrix Anal. Appl., **9**, 61–76.

Beylkin, G., 1995, On the fast Fourier transform of functions with singularities: Appl. Comp. Harm. Anal., **2**, no. 4, 363–381.

Bhattacharyya, B., 1966, Continous spectrum of the total-magnetic-field anomaly due to a rectangular prismatic body: Geophysics, **31**, no. 1, 97–121.

Bitmead, R., and Anderson, B., 1980, Asymptotically fast solution of Toeplitz and related systems of linear equations: Lin. Alg. Appl., **34**, 103–117.

Briggs, I., 1974, Machine contouring using minimum curvature: Geophysics, **39**, no. 1, 39–48.

Chan, R., and Strang, G., 1989, Toeplitz equations by conjugate gradients with circulant preconditioner: SIAM J. Sci. Stat. Comput., **10**, 104–119.

Cordell, L., 1992, A scattered equivalent-source method for interpolation and gridding of potential field data in three dimensions: Geophysics, **57**, no. 4, 629–636.

Feichtinger, H. G., and Gröchenig, K., 1994, Theory and practice of irregular sampling *in* Benedetto, J., and Frazier, M., Eds., Wavelets: Mathematics and Applications:: CRC Press, 305–363.

Feichtinger, H. G., and Strohmer, T., 1993, Fast iterative reconstruction of band-limited images from irregular sampling values , Proc. on Computer Analysis of Images and Patterns, 82–91.

Feichtinger, H. G., Gröchenig, K., and Strohmer, T., 1995, Efficient numerical methods in non-uniform sampling theory: Numerische Mathematik, **69**, 423–440.

Foley, T., and Hagen, H., 1994, Advances in scattered data interpolation: Surv. Math. Ind., **4**, 71–84.

Golub, G., and van Loan, C., 1996, Matrix computations, third ed.: Johns Hopkins, London, Baltimore.

Granser, H., Steinhauser, P., Ruess, D., and Meurers, B., 1991, Beiträge zur Erkundung der Untergrundstrukturen der Neusiedlersee-Region mit gravimetrischen und magnetischen Methoden: Mitteilungen der Österreichischen Geologischen Gesellschaft, **84**, 223–238.

Gröchenig, K., 1994, Irregular sampling, Toeplitz matrices, and the approximation of entire functions of exponential type, preprint.

Gunn, P., 1975, Linear transformations of gravity and magnetic field: Geophysical Prospecting, **23**, 300–312.

Hageman, L., and Young, D., 1981, Applied iterative methods: Academic Press.

Hansen, R., 1993, Interpretive gridding by anisotropic kriging: Geophysics, **58**, no. 10, 1491–1497.

Higgins, J., 1996, Sampling theory in Fourier and signal analysis: Foundations: Oxford University Press.

Robinson, E., and Treitel, S., 1980, Geophysical signal analysis: Prentice Hall, Englewood Cliffs, N.J.

Scherzer, O., 1996, A multi-scale algorithm for solving nonlinear ill-posed problems, preprint.

Strang, G., 1986, A proposal for Toeplitz matrix calculations: Stud. Appl. Math., **74**, 171–176.

Strohmer, T., 1996, Computationally attractive reconstruction of band-limited images from irregular samples: IEEE Trans. on Image Processing, to appear.

Webring, M., 1981, MINC: a gridding program based on minimum curvature: U.S.Geol. Surv. Open-File Rep., **81-1230**.